Chapter 1
Stable Extrapolation of Field Produced by Volumetric Magnetizations

Juliette Leblond, Mubasharah Khalid Omer and Dmitry Ponomarev

Abstract In the particular setup of the planar scanning Superconducting Quantum Interference Device (SQUID), the vertical component of the magnetic field produced by a magnetized sample is measured. Recovering the sample's internal magnetization from this measured data, an inverse problem that is central in the field of paleomagnetism, is a severely ill-posed process. Moreover, standard recovery methods are further hindered by limited measurements and the noise therein. To address these issues, we develop a method to simultaneously extrapolate and denoise the field data, thereby solving a preliminary inverse problem for an auxiliary function of the magnetization. The proposed approach is based on a regularization framework that exploits an explicit field-magnetization relation. To encode the harmonic structure of the problem, we construct a set of basis functions derived from spherical harmonics via the Kelvin transform. The method is applicable to both volumetric and planar magnetization distributions.

Key words: Inverse problems; measurement extrapolation/extension; paleomagnetism; regularization.
MSC2020: 31B20; 35J05; 35R25; 35R30; 41A29; 41A30; 42B37; 47A52.

1.1 Introduction

Deducing the magnetization of geological samples holds significant importance in the field of paleomagnetism. In the particular setup we consider, the vertical component of the magnetic field above a thin rock sample is measured using a SQUID mi-

M. K. Omer
e-mail: mubasharah.omer@inria.fr

D. Ponomarev, J. Leblond
e-mail: dmitry.ponomarev@inria.fr, juliette.leblond@inria.fr
FACTAS, Inria Center at Université Côte d'Azur, France

croscope, on a limited, planar region. However, recovering the magnetization from these measurements is an ill-posed inverse problem, in particular, due to the non-uniqueness of the solution [1]. Various methods of estimation of the magnetization distribution could be applied depending on specific assumptions, such as unidirectionality, sparsity, or smoothness [2, 3], yet, across these techniques, a significant challenge arises due to measurements' limited area and noise pollution. The resulting instability can be narrowed, for example, by extending the measured field data through extrapolation techniques [4]. Moreover, asymptotic formulas allow recovery of the net magnetization moment from field measurements on a large planar area, with accuracy improving as the measurement size increases [5], further motivating extrapolation of measured field data.

By shifting the objective from full magnetization recovery to magnetic field extrapolation, we target a problem that is less ill-posed; in the absence of noise, the extrapolated field exists and is unique [4]. Still, small perturbations in the data may produce large deviations in the extrapolation, and although a noise-free data-set gives a unique extension, real data contain noise. Regularization is thus required to stabilize the extrapolation, and acts as a denoising mechanism within the measurement region. Consequently, the aim of the present work is to extrapolate the measured field to a larger planar domain beyond the measurement area, while simultaneously denoising it within the measurement region.

Using the field-source relations established in Section 1.2, Section 1.3 describes an approach to the field extrapolation issue as a constrained least-squares problem for a function of the magnetization. Section 1.4 presents a projection-based solution method, develops a basis for its implementation via the Kelvin transform of spherical harmonics, and introduces an alternative basis for performance comparison. Numerical results are presented in Section 1.5.

1.2 Magnetization and induced magnetic field

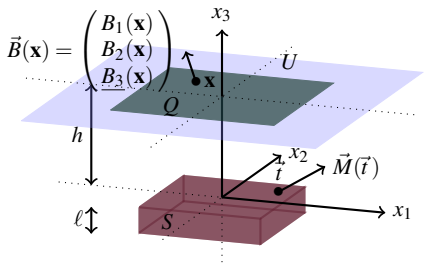

Fig. 1.1 Schematic description of the geometrical setting and notations.

We describe the SQUID microscope setup (schematized in Fig. 1.1), that measures the vertical component of the magnetic field B_3 on a horizontal planar region $Q \subset \mathbb{R}^2$ at height $h > 0$, in the upper half-space $\mathbb{H} = \{\vec{x} = (x_1, x_2, x_3)^T \in \mathbb{R}^3 : x_3 > 0\}$. The magnetization $\vec{M} = (M_1, M_2, M_3)^T \in (L^2(\mathbb{R}^3))^3$ is supported in the compact domain $S = [-s, s]^2 \times [-\ell, 0] \subset \mathbb{R}^3$ with $s, \ell > 0$. We introduce a larger region $U \subseteq \mathbb{R}^2$, with $U \supset Q$, to which measurements of B_3 will be extended. We work in the complex Hilbert spaces $L^2(\mathbb{R}^2)$ and $L^2(Q)$, equipped with the standard inner products:

$$\langle f, g \rangle_{L^2(\mathbb{R}^2)} = \iint_{\mathbb{R}^2} f(\mathbf{x}) \overline{g(\mathbf{x})} \mathrm{d}\mathbf{x} \quad \text{and} \quad \langle f, g \rangle_{L^2(Q)} = \iint_{Q} f(\mathbf{x}) \overline{g(\mathbf{x})} \mathrm{d}\mathbf{x}.$$

Their associated norms will be denoted by $\|f\|_{L^2(\mathbb{R}^2)}$ and $\|f\|_{L^2(Q)}$.

To relate the field to the underlying magnetization, we use Maxwell's equations in the quasi-static regime, assuming no time dependence and the absence of free currents. Under these assumptions the magnetic field derives from a scalar potential Φ [1], which satisfies

$$\Delta \Phi = \nabla \cdot \vec{M} \quad \text{in } \mathbb{R}^3.$$

For $\vec{x} \in \mathbb{R}^3 \setminus \mathrm{supp}(\vec{M})$, with $*_{3\mathrm{d}}$ denoting the 3d convolution, this yields:

$$\Phi(\vec{x}) = \left(-\frac{1}{4\pi|\vec{t}|} *_{3\mathrm{d}} (\nabla \cdot \vec{M}) \right)(\vec{x}) = -\frac{1}{4\pi} \iiint_{\mathbb{R}^3} \frac{\nabla \cdot \vec{M}(\vec{t})}{|\vec{x} - \vec{t}|} \mathrm{d}\vec{t}. \tag{1.1}$$

Since the SQUID measures the vertical field component B_3, we use the relation

$$B_3 = -\mu_0 \partial_{x_3} \Phi \quad \text{in } \mathbb{H}, \tag{1.2}$$

where μ_0 is the magnetic permeability constant. Using Eq. (1.1) in (1.2), we write

$$B_3 = -\frac{\mu_0}{2} \sum_{j=1}^{3} \left(\partial_{x_j} p_{\mathbb{H}} *_{3\mathrm{d}} M_j \right) \quad \text{in } \mathbb{H}, \tag{1.3}$$

where, for all $\vec{x} \in \mathbb{H}$, $p_{\mathbb{H}}(\vec{x}) = x_3 / \left(2\pi|\vec{x}|^3\right)$ denotes the Poisson kernel in $\mathbb{H}$.

To simplify (1.3), we use the identity [1, Eq. (12)]: for all $g \in L^2(\mathbb{R}^2)$ and $j = 1, 2$,

$$\partial_{x_j} p_{\mathbb{H}} *_{2\mathrm{d}} g = \partial_{x_3} p_{\mathbb{H}} *_{2\mathrm{d}} R_j[g],$$

where $*_{2\mathrm{d}}$ denotes the 2d convolution with respect to the first two components, and R_j represent the 2d Riesz transforms defined as, for all $\mathbf{x} = (x_1, x_2)^T \in \mathbb{R}^2$,

$$R_j[g](\mathbf{x}) = \frac{1}{2\pi} \lim_{\varepsilon \to 0^+} \iint_{\mathbb{R}^2 \setminus \mathbb{D}_\varepsilon(\mathbf{x})} \frac{(x_j - t_j) g(\mathbf{t})}{|\mathbf{x} - \mathbf{t}|^3} \mathrm{d}\mathbf{t},$$

with $\mathbf{t} = (t_1, t_2)^T$, and $\mathbb{D}_\varepsilon(\mathbf{x}) = \{\mathbf{y} \in \mathbb{R}^2 : |\mathbf{y} - \mathbf{x}| < \varepsilon\}$, $\varepsilon > 0$. We thus obtain:

$$B_3(\mathbf{x}, x_3) = -\frac{\mu_0}{2} \left[\partial_{x_3} p_{\mathbb{H}}(\cdot, x_3) *_{2\mathrm{d}} f_M(\cdot) \right](\mathbf{x}), \tag{1.4}$$

where

$$f_M(\mathbf{x}) = \int_{-\ell}^{0} (p_{\mathbb{H}} *_{2\mathrm{d}} \tilde{f}_M)(\mathbf{x}, -t_3)\mathrm{d}t_3,$$

with $\tilde{f}_M(\mathbf{t},t_3) = \sum_{j=1}^{2} R_j[M_j(\cdot,t_3)](\mathbf{t}) + M_3(\mathbf{t},t_3)$, and $f_M \in L^2(\mathbb{R}^2)$, as Riesz transforms are bounded operators on $L^2(\mathbb{R}^2)$ [6, Ch. III]. The above relation for volumetric magnetizations readily adapts to planar magnetizations with $f_M \equiv \tilde{f}_M$.

1.3 Field extrapolation problem

The field extrapolation proceeds in two steps. We first estimate f_M appearing in Eq. (1.4) by solving the associated inverse problem. Then, we apply a suitable operator to this estimate to obtain the extrapolated field component B_3^{ext}, on $U \supset Q$.

Motivated by Eq. (1.4), we introduce the bounded, linear operator, $\mathscr{B} : L^2(\mathbb{R}^2) \to L^2(Q)$, so that for all $f \in L^2(\mathbb{R}^2)$ and for a fixed $x_3 = h$, where h corresponds to the height of the measurement (and extrapolation) plane (see Fig. 1.1),

$$\mathscr{B}f = -\frac{\mu_0}{2}\left[\partial_{x_3} p_{\mathbb{H}}\Big|_{x_3=h} *_{2\mathrm{d}} f\right]\Big|_Q,$$

whence, for exact measured data, for $\mathbf{x} \in Q$, $B_3^{\mathrm{meas}}(\mathbf{x},h) = \mathscr{B}f_M(\mathbf{x})$. The adjoint operator, $\mathscr{B}^* : L^2(Q) \to L^2(\mathbb{R}^2)$, is defined as, for all $g \in L^2(Q)$,

$$\mathscr{B}^* g = -\frac{\mu_0}{2}\partial_{x_3} p_{\mathbb{H}}\Big|_{x_3=h} *_{2\mathrm{d}} (\chi_Q g),$$

where χ_Q is the characteristic function of Q.

From the vanishing property of real-analytic functions [9, Th. 1.27], we can deduce that $\mathrm{Ker}(\mathscr{B}^*) = \{0\}$. It follows that $\overline{Ran(\mathscr{B})} = L^2(Q)$ [8, Th. 5.22.6]. Hence, for $B_3^{\mathrm{meas}} \in L^2(Q)$, there exists a minimizing sequence $(f_n)_{n\in\mathbb{N}} \in L^2(\mathbb{R}^2)$ such that $\|B_3^{\mathrm{meas}} - \mathscr{B}f_n\|_{L^2(Q)} \underset{n\to+\infty}{\longrightarrow} 0$. However, $\|f_n\|_{L^2(\mathbb{R}^2)} \underset{n\to+\infty}{\longrightarrow} \infty$ when $B_3^{\mathrm{meas}} \notin Ran(\mathscr{B})$. So, a norm constraint is crucial whenever $B_3^{\mathrm{meas}} \notin Ran(\mathscr{B})$, which is always the case when data consist of noisy measurements. We thus consider the following constrained approximation problem to estimate f_M:

Problem 1 Given $B_3^{\mathrm{meas}} \in L^2(Q)$ and $C > 0$, find $f \in L^2(\mathbb{R}^2)$ such that

$$\min_{f\in L^2(\mathbb{R}^2)} \|B_3^{\mathrm{meas}} - \mathscr{B}f\|_{L^2(Q)} \text{ subject to } \|f\|_{L^2(\mathbb{R}^2)} \leq \mathrm{C}.$$

Theorem 1 *Let $B_3^{\mathrm{meas}} \in L^2(Q) \setminus \mathrm{Ran}(\mathscr{B})$. For a given $C > 0$, there exists a $\lambda > 0$ such that the unique solution $f^\lambda \in L^2(\mathbb{R}^2)$ of Problem 1 satisfies*

$$\mathscr{B}^*\mathscr{B}f^\lambda + \lambda f^\lambda = \mathscr{B}^* B_3^{\mathrm{meas}} \quad \text{in } \mathbb{R}^2, \tag{1.5}$$

and $\|f^\lambda\|_{L^2(\mathbb{R}^2)} = \mathrm{C}$.

Remark: If $B_3^{\text{meas}} \in \text{Ran}(\mathscr{B})$, the constraint in Problem 1 is inactive and the corresponding solution satisfies $\lambda = 0$.

The proof of Theorem 1 follows from application of [7, Th. 4.6].

1.4 Solution approach

We adopt a projection method, approximating the infinite-dimensional problem in $L^2(\mathbb{R}^2)$ by a finite-dimensional one in $\mathrm{V}_J^\varphi = \text{span}\{\{\varphi_j\}_{j=1,\dots,J}\}$ for $J \in \mathbb{N}$, where $\{\varphi_j\}_{j=1,\dots,J}$ is an arbitrary set of orthonormal basis functions on $L^2(\mathbb{R}^2)$:

$$f^\lambda \approx \sum_{j=1}^{J} c_j \varphi_j, \qquad \mathscr{B}^* B_3^{\text{meas}} \approx \sum_{j=1}^{J} d_j \varphi_j,$$

with $(c_j)_{j=1,\dots,J} \in \mathbb{R}^J$, and the known coefficients, for $j = 1, \dots, J$,

$$d_j = \langle \mathscr{B}^* B_3^{\text{meas}}, \varphi_j \rangle_{L^2(\mathbb{R}^2)} = \langle B_3^{\text{meas}}, \mathscr{B}\varphi_j \rangle_{L^2(Q)}.$$

We project equation (1.5) orthogonally onto V_J^φ: for $k = 1, \dots, J$,

$$\sum_{j=1}^{J} \Big(\langle \mathscr{B}^* \mathscr{B} \varphi_j, \varphi_k \rangle_{L^2(\mathbb{R}^2)} + \lambda \, \delta_{j,k} \Big) c_j = d_k, \tag{1.6}$$

where $\delta_{j,k}$ is the Kronecker symbol. Note that the matrix $\langle \mathscr{B}^* \mathscr{B} \varphi_j, \varphi_k \rangle_{L^2(\mathbb{R}^2)} = \langle \mathscr{B}\varphi_j, \mathscr{B}\varphi_k \rangle_{L^2(Q)}$ is symmetric and positive definite and, with $\lambda > 0$, the system (1.6) is uniquely solvable. The solution coefficients c_j are subsequently used to compute the extrapolated magnetic field component, using that $f_M \approx f^\lambda$ in Eq. (1.4):

$$B_3^{\text{ext}} \approx -\frac{\mu_0}{2} \sum_{j=1}^{J} c_j \partial_{x_3} p_{\mathbb{H}} \Big|_{x_3 = h} *_{2\text{d}} \varphi_j \quad \text{in } \mathbb{R}^2.$$

Note that $B_3^{\text{ext}}|_Q$ yields denoised reconstruction of B_3^{meas}. Indeed, since $\lambda > 0$, the minimizer in the constrained problem is prevented from reproducing the rapid fluctuations (noise) in B_3^{meas}.

We now propose two choices of bases $\{\varphi_j\}$:

- **Kelvin-transformed spherical harmonics**

The Kelvin transform [9, Ch. 4] of spherical harmonics gives a basis on $L^2(\mathbb{R}^2)$, preserving smoothness, algebraic decay, and orthogonality of the spherical harmonics on $L^2(\mathbb{S})$. As these functions arise as 2d traces of harmonic functions in 3d, they are naturally compatible with our setting; $\mathscr{B}^* B_3^{\text{meas}}$ is the trace on $\mathbb{R}^2$ of a harmonic function in the upper half-space and decays algebraically. This suggests that this basis may yield accurate approximations of such targets with relatively few functions.

The spherical harmonics are defined as, for $0 \le \theta \le \pi$, $0 \le \phi \le 2\pi$, [10, Ch. 14]

$$Y_{l,m}^{\mathbb{S}}(\theta,\phi)=\frac{(-1)^{l+m}}{2^l l!}\left(\frac{(l-m)!(2l+1)}{4\pi(l+m)!}\right)^{\frac{1}{2}}e^{im\phi}(\sin\theta)^m\left(\frac{\mathrm{d}}{\mathrm{d}(\cos\theta)}\right)^{l+m}(\sin\theta)^{2l},$$

where their degree l and order m are such that $l\in\mathbb{N}\cup\{0\}$ and $|m|\leq l$.

To derive an $L^2(\mathbb{R}^2)$-basis from the spherical harmonics, we start by considering a transformation based on inversion with respect to an auxiliary sphere of radius $\sqrt{2}$ centered at $\vec{x}_0=(0,0,-1)$: for all $\vec{x}\in\mathbb{S}\setminus\{\vec{x}_0\}$,

$$T(\vec{x})=\vec{x}_0+2\frac{\vec{x}-\vec{x}_0}{|\vec{x}-\vec{x}_0|^2},$$

which maps the unit sphere $\mathbb{S}$ to the plane $\mathbb{R}^2$ (at height 0), and back [9, Ch. 7]. Then, for a function $f\in L^2(\mathbb{S})$, the Kelvin transform $\mathscr{K}$ is defined as: for all $\mathbf{x}\in\mathbb{R}^2$,

$$\mathscr{K}[f](\mathbf{x})=\sqrt{\frac{2}{|\mathbf{x}|^2+1}}f(T(\mathbf{x},0)),$$

and is an isometry between $L^2(\mathbb{S})$ and $L^2_\omega(\mathbb{R}^2)$, where $\omega(\mathbf{x})=(|\mathbf{x}|^2+1)^{-1}$. We then define the so-called Kelvin-transformed spherical harmonics, for all $\mathbf{x}\in\mathbb{R}^2$,

$$S_j(\mathbf{x})=\frac{1}{\sqrt{|\mathbf{x}|^2+1}}\mathscr{K}[Y_j^{\mathbb{S}}](\mathbf{x}),$$

where we have used $j=l^2+l+m+1$, with $l=\lfloor\sqrt{j-1}\rfloor$ and $m=j-\left(\lfloor\sqrt{j-1}\rfloor^2+\lfloor\sqrt{j-1}\rfloor+1\right)$. The functions $\{S_j\}_{j\in\mathbb{N}}$ form an orthonormal system in $L^2(\mathbb{R}^2)$.

- **Malmquist-Takenaka basis**

The Malmquist-Takenaka (MT) rational functions form an orthonormal basis of $L^2(\mathbb{R})$ with algebraic decay [11]. In 1d they are given by, for $n\in\mathbb{Z}$ and $x\in\mathbb{R}$,

$$\vartheta_n(x)=\sqrt{\frac{2}{\pi}}\,i^n\left(\frac{1+2ix}{1-2ix}\right)^n\frac{1}{1-2ix}.$$

We extend the MT basis to $L^2(\mathbb{R}^2)$, as a product of the 1d functions i.e. for $n,m\in\mathbb{Z}$,

$$\psi_{n,m}(\mathbf{x})=\vartheta_n(x_1)\vartheta_m(x_2).$$

The family $\{\psi_{n,m}\}_{n,m\in\mathbb{Z}}$ forms an orthonormal basis of $L^2(\mathbb{R}^2)$. We index the 2d MT functions by ordering $(n,m)\in\mathbb{Z}^2$ in nondecreasing values of $\sqrt{n^2+m^2}$, obtaining a single-indexed family $\{\psi_j\}_{j\in\mathbb{N}}$ whose oscillations increase with j.

1.5 Numerical results and outlook

We investigate the following hypothesis: Kelvin-transformed spherical harmonics provide more accurate approximations of algebraically-decaying targets, which are 2d traces of harmonic functions, than the 2d MT system of the same dimension.

Numerical simulations are performed in MATLAB for a specific magnetization $\vec{M}$ supported on S, with $s = 1$ and $\ell = 0.2$, i.e. for all $\vec{t} \in S$,

$$\vec{M}(\vec{t}) = \begin{pmatrix} t_3((t_3+\ell)(t_1^2-s)^2 + 4(t_1^2-s)(t_3+\ell)^2)(t_2^2-s)^2 \\ t_3((t_3+\ell)(t_2^2-s)^2 + 4(t_3+\ell)(t_2^2-s))(t_1^2-s)^2 \\ t_3(t_3+\ell)(t_1^2-s)^2(t_2^2-s)^2 \end{pmatrix}.$$

We synthetically generate B_3^{meas} from $\vec{M}$, using Eq. (1.3) with $\mu_0 = 1$. For this data, we conduct the described reconstruction scheme using the fixed height $h = 1$, measurement region $Q = [-1,1]^2$ and extrapolation region $U = [-10,10]^2$. Note that the data is numerically generated and free of experimental noise. However, the solution's projection onto the finite-dimensional subspace, and quadrature errors in the computation of B_3^{meas}, introduce computational artifacts, creating numerical noise.

Using the Kelvin-transformed spherical harmonics, we first consider the approximation space $\mathrm{V}_J^S = \operatorname{span}\{S_1, \ldots, S_J\}$, for a modest $J = 81$. The regularization parameter λ is chosen via the L-curve method [12], we balance data-fidelity and solution-size by choosing λ corresponding to the corner of the curve (Fig. 1.2 (left)). The results are shown in Fig. 1.2; the relative L^2-error is on the order $\mathscr{O}(10^{-6})$ in the measured region and $\mathscr{O}(10^{-2})$ in the extrapolated region.

We now consider the approximation space $\mathrm{V}_J^\Psi = \operatorname{span}\{\psi_1, \ldots, \psi_J\}$, spanned by the MT basis, and the same dimension $J = 81$. The results are shown in Fig. 1.3, corresponding to the λ chosen via the L-curve method. The relative L^2-error is on the order $\mathscr{O}(10^{-5})$ in the measured region and $\mathscr{O}(10^{-1})$ in the extrapolated region.

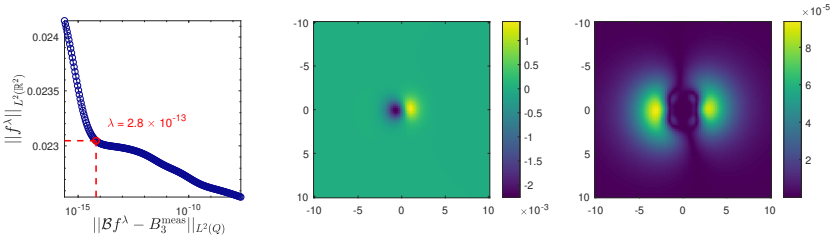

Fig. 1.2 L-curve for the deduction of λ (left), B_3^{ext} obtained using the approximation in V_J^S (center) and the pointwise error between the true magnetic field on U and B_3^{ext} (right).

Thus, for identical number of functions, the Kelvin-transformed spherical harmonics provide a more accurate reconstruction and extrapolation than the MT ba-

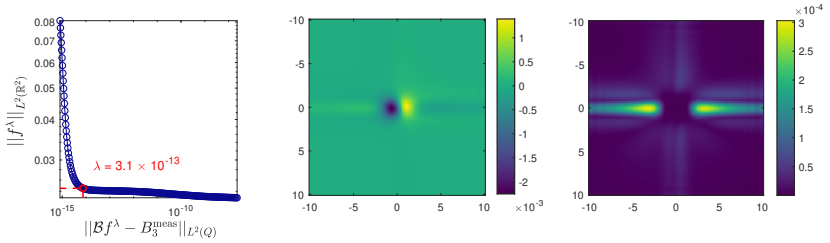

Fig. 1.3 L-curve for the deduction of λ (left), B_3^{ext} obtained using the approximation in V_J^{Ψ} (center), and the pointwise error between the true magnetic field on U and B_3^{ext} (right).

sis. This supports the hypothesis that a basis adapted to the harmonic structure, in addition to the decay, of the problem delivers better approximations with the same number of functions. Future work will investigate the robustness of this advantage on noisy experimental data, and will use the reconstructed magnetization function (f_M) to infer magnetization components.

References

1. Baratchart, L., Chevillard, S., Leblond, J.: Silent and equivalent magnetic distributions on thin plates. Theta Series in Advanced Mathematics, **Vol**(22) (2016).
2. Egli, R., Heller, F.: High-resolution imaging using a high-T_c superconducting quantum interference device (SQUID) magnetometer. Journal of Geophysical Research, **Vol**(105) (2000).
3. Weiss, B. P., Lima, E., Fong, L., Baudenbacher, F.: Paleomagnetic analysis using SQUID microscopy. Journal of Geophysical Research, **Vol**(112) (2007).
4. Ponomarev, D.: A method to extrapolate the data for the inverse magnetisation problem with a planar sample. In: Hasanoğlu, A. H., Novikov, R., Bockstal, K. V. (eds.) Inverse Problems: Modeling and Simulation - IPMS Conference 2024. Birkhäuser, Cham (2025).
5. Ponomarev, D.: Magnetisation moment of a bounded 3D sample: asymptotic recovery from planar measurements on a large disk. Journal of Computational and Applied Mathematics, **Vol**(476) (2026).
6. Stein, E. M.: Singular Integrals and Differentiability Properties of Functions. Princeton University Press (1971).
7. Angell, T. S., Kirsch, A.: Optimization Methods in Electromagnetic Radiation. Springer Monographs in Mathematics (2004).
8. Naylor, A. W., Sell, G. R.: Linear Operator Theory in Engineering and Science. Springer New York (1982).
9. Axler, S., Bourdon, P., Ramey, W.: Harmonic Function Theory. Springer New York (2001).
10. Olver, F. W. J., Lozier, D. W., Boisvert, R. F., Clark, C. W.: The NIST Handbook of Mathematical Functions. Cambridge University Press (2010).
11. Iserles, A., Webb, M.: A family of orthogonal rational functions and other orthogonal systems with a skew-Hermitian differentiation matrix. Journal of Fourier Analysis and Applications **Vol**(26) (2020).
12. Hansen, P. C.: The L-Curve and its use in the numerical treatment of inverse problems. Computational Inverse Problems in Electrocardiology, **Vol**(4) (2001).